

“Block-in-matrix” fabrics that lack shearing but possess composite cleavage planes: A sedimentary *mélange* origin for the Yuwan accretionary complex in the Ryukyu island arc, Japan

Soichi Osozawa^{1,†}, Junpei Morimoto¹, and Martin F.J. Flower²

¹*Department of Earth Sciences, Graduate School of Science, Tohoku University, Sendai 980-8578, Japan*

²*Department of Earth and Environmental Sciences, University of Illinois at Chicago, Chicago, Illinois 60607-7059, USA*

ABSTRACT

While *mélanges* have been taken to be a significant component of accretionary complexes, the use of this term has been mostly descriptive, given the lack of consensus concerning their genesis. However, many workers have interpreted asymmetric shear fabrics in *mélanges* as evidence of a tectonic origin (i.e., giving rise to tectonic *mélanges*), in contrast to olistostromes, which are considered to be purely sedimentary in origin due (at least in part) to the lack of such shear fabrics. It is still uncertain whether accretionary processes include those that involve the intense shearing of oceanic lithologies along with, for example, the incorporation and entrapment of exotic blocks by muddy matrices during sediment deposition and deformation in axial deep-sea trench settings. Here, we argue that the so-called “block-in-matrix” fabrics that characterize accretionary complexes are primarily sedimentary in origin and are distinct from shear fabrics represented by tectonic *mélanges*. We also propose that, following their accretion, subsequent recycling of such “oceanic” materials is a common feature within evolving accretionary prisms. Lastly, we draw attention to the observation that D1 pressure-solution cleavage planes—notably widespread in the lower Cretaceous Yuwan complex, Amami Oshima Island, in the Ryukyu arc, SW Japan—are absent from the minor asymmetric shear structures that often characterize tectonic *mélanges*. In contrast, we suggest that the Yuwan complex represents the effects of broadly symmetric flattening. This scenario is supported by our observation that the number of sedimentary and deformation events differs significantly compared to the single phase of shearing

expected in tectonic *mélanges*. D minus 1 (D_{-1}) pressure-solution and axial-planar cleavages are only observed in exotic blocks and exhibit older accretionary deformation events within a preexisting accretionary prism. Of the existing structural associations, Sd1 is the oldest, predating the D_{-1} sedimentary episode, and it represents an oceanic sedimentary phase associated with the formation of a distinct type of block-in-matrix fabric produced by the accumulation of debris flows at seamount margins. Sd2 represents a succeeding sedimentary episode characterized by trench-axis debris flow, including oceanic inclusions derived from collapsed material from an older accretionary prism. The resulting Sd2 block-in-matrix fabric is one of the main lithologic components of the Amami Oshima Yuwan complex. Here, the Sd2 episode typically includes an igneous fabric, consisting of nonexotic intrusive and extrusive basalts within a terrigenous matrix, suggesting that the Yuwan prism may have also been associated with a trench-trench-ridge triple junction. D1 coaxial deformation is observed to overprint all of the episodes represented, although it has not destroyed or significantly sheared their respective fabrics, especially in regard to the main Sd2 block-in-matrix structures, which are therefore considered to represent original sedimentary structures.

INTRODUCTION

Since the term *mélange* was applied by Hsü (1968) in relation to the Franciscan Complex of the California Coast Range, the coexistence of *mélange* and blueschist lithologies (e.g., Ernst, 1988) has implied the existence of a former subduction zone. It was later observed that blueschist lithologies were not always common in ancient worldwide accretionary complexes, and that the existence of a *mélange* is one of

the most important criteria for identifying such subduction-related complexes. *Mélange*, or block-in-matrix fabric, was defined by Cowan (1985) as the presence of inclusions of diverse shape and size chaotically dispersed in a fine-grained matrix. However, models for the genesis of *mélange* have been controversial, variously including one or another of three different conceptual mechanisms: olistostromal deposition (e.g., Brandon, 1989; Pini, 1999), mud diapirism (e.g., Orange, 1990), and tectonic shearing (e.g., Cloos, 1982), or combinations of these. In consequence, the genesis of chaotic fabrics continues to be a subject of debate.

In the case of Japanese accretionary complexes, where block-in-matrix fabric has been observed, these lithological assemblages have been referred to as *mélange*, especially in the Cretaceous Shimanto zone (Taira et al., 1988). Between the late 1970s and early 1980s, the genesis of such *mélanges* was generally considered in terms of mass wasting (in most cases, olistostromes) on the outer slopes of deep-sea trenches and olistostromes in axial regions that might have been expected to accumulate host terrigenous and exotic oceanic lithologies (Taira et al., 1982).

By the late 1980s, however, new observations along with the discovery of consistently asymmetric shear fabric—at first in Alaska and the Aleutians (e.g., Fisher and Byrne, 1987)—led to the interpretation of tectonic *mélanges* in terms of large-scale shear banding in response to, and connected with, processes of underplating (Needham, 1987; Kimura and Mukai, 1991; Taira et al., 1992; Onishi and Kimura, 1995; Hashimoto and Kimura, 1999). According to this type of interpretation, all geological zones attributed to olistostrome-forming processes could be reinterpreted as tectonic *mélanges*. Accepting the concept of “tectonic *mélange*,” recent papers concerning Japanese accretionary complexes have focused on metamorphic

[†]E-mail: osozawa@m.tains.tohoku.ac.jp.

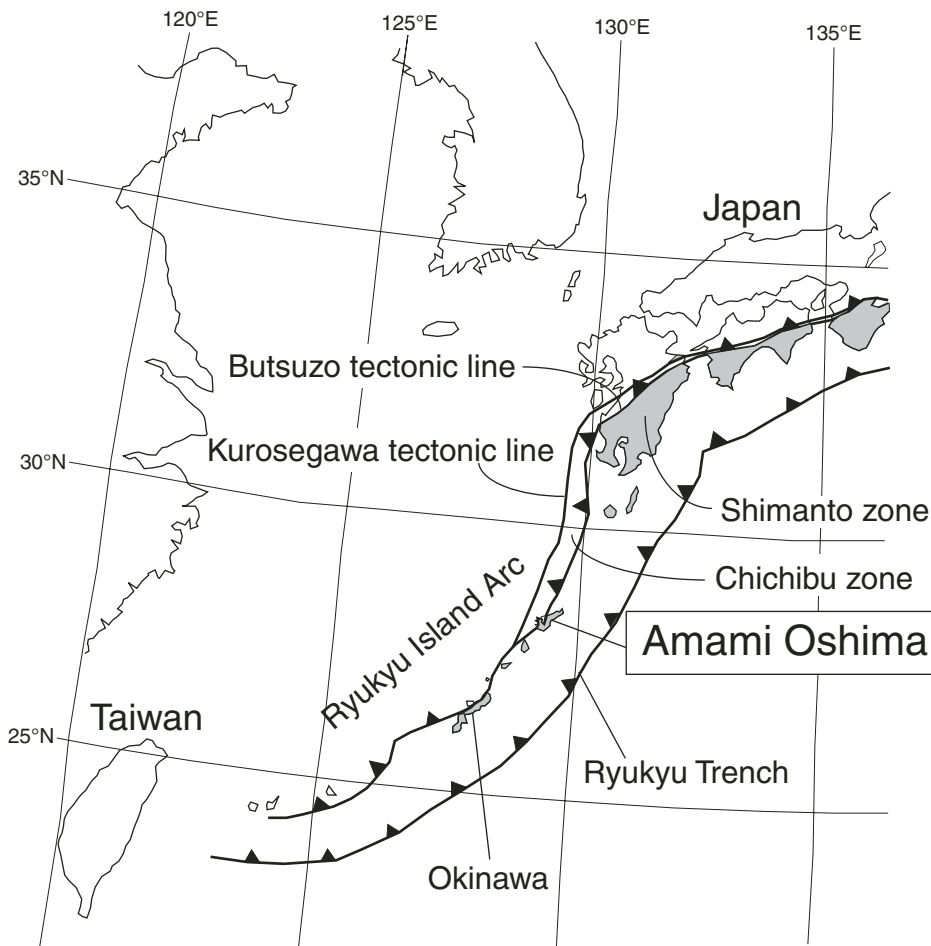


Figure 1. Index map of Amami Oshima Island.

pressure-temperature (P - T) paths associated with mélanges and major thrusting mechanisms associated with giant earthquakes (e.g., Ikesawa et al., 2005).

Several studies of Japanese mélanges have noted some conflict with the tectonic mélange model. Inclusions and matrix of some block-in-matrix fabrics are only oceanic rocks of chert, limestone, and basalt, which as a whole constitute a block within additional block-in-terrigeneous matrix fabric. The former fabric was formed by a mass wasting process in an open-ocean setting, prior to and independent of the main phase of extensive accretion (Osozawa, 1986; Matsuda and Ogawa, 1993). Clastic dikes truncating exotic blocks are not rare in such Japanese mélanges (e.g., Osozawa, 1984; Hibbard et al., 1992), and they indicate that the matrix was unconsolidated and water-saturated, which led some authors to conclude that the mélanges were formed as a result of mud diapirism (e.g., Wakita, 1988).

While some mélanges are occasionally associated with basalt intrusive activity, and the pre-

served chill margins may be observed (Osozawa et al., 1990; Osozawa, 1993; Kiminami et al., 1994; Osozawa and Yoshida, 1997), there is little or no indication that the original igneous structures have been perturbed by the expected intense shearing. In some cases, mélanges clearly represent lithologic components inter-layered with coherent hemipelagic and terrigenous units (e.g., Taira et al., 1992; Osozawa, 1993; Osozawa et al., 2004). This scenario might appear to require stratigraphic shear stress to be concentrated, particularly in the horizontal plane, to allow the formation of a mélange layer, although this process remains conjectural. While asymmetric shear fabric is not apparent in some mélanges (Osozawa et al., 1990, 2004), it has been recognized independently in other accretionary complexes that lack block-in-matrix fabric (Needham, 1987; Schoonover and Osozawa, 2004).

In attempting to reconcile these diverse, and apparently conflicting, observations and interpretations bearing on mélange genesis, we present field and petrographic evidence from the

Yuwan complex of the Ryukyu island arc. On the basis of our results, we show that the Yuwan mélange was formed essentially by a combination of sedimentary and (subsidiary) tectonic processes accompanied by recycling of older accretionary prism material.

GEOLOGICAL SETTING

The Amami Oshima Island lies in the central part of the Ryukyu island arc, most of the associated accretionary complex considered to be continuous with the Shimanto zone of the southwest Japanese arc system (Schoonover and Osozawa, 2004; Fig. 1).

The accretionary complex has been divided into four parts (Figs. 1 and 2): the early Cretaceous–Barremian Yuwan complex, the middle Cretaceous–Albian Odana complex, the Cenomanian Naze complex, and the Turonian Ogachi complex, which represent both upper and lower structural components in western and central Amami Oshima. These ages, based mostly on radiolarian fossil evidence (Osozawa, 1984) have been refined and modified by Osozawa and Yoshida (1997). Only the Yuwan complex correlates with the southwest Japanese Chichibu zone, while the others belong structurally to the Shimanto zone.

The focus of the present paper is the Yuwan complex in western Amami Oshima, which is the structurally highest and overlies the Odana complex (Fig. 2). The Odana complex, in turn, structurally overlies the Naze complex, which is most widely distributed over western and central Amami Oshima (Figs. 1 and 2). The Naze complex also tectonically overrides the Ogachi complex, although farther east, the Ogachi complex also overlies the other Naze complex, distributed in eastern Amami Oshima (Fig. 2). The Amami Oshima accretionary complexes were accreted progressively from west to east in response to westward subduction, suggesting that the eastern part of the complex is slightly younger than the structurally higher western and central parts; the combined succession is referred to as the Naze complex, given the presence of the same lithologic assemblages in each component (Osozawa, 1984). However, no diagnostic radiolarian fossils have been obtained from the eastern complex. The remaining part of Amami Oshima is the Paleogene–Eocene Wano Formation, which evolved as a forearc basin at the eastern end of Amami Oshima (Fig. 2; Osozawa, 1984; Osozawa and Yoshida, 1997). With the exception of the Wano Formation, each of the complexes was intruded by postaccretionary Eocene granites.

The Yuwan complex (Fig. 2) forms a Barremian volcanic and sedimentary succession that

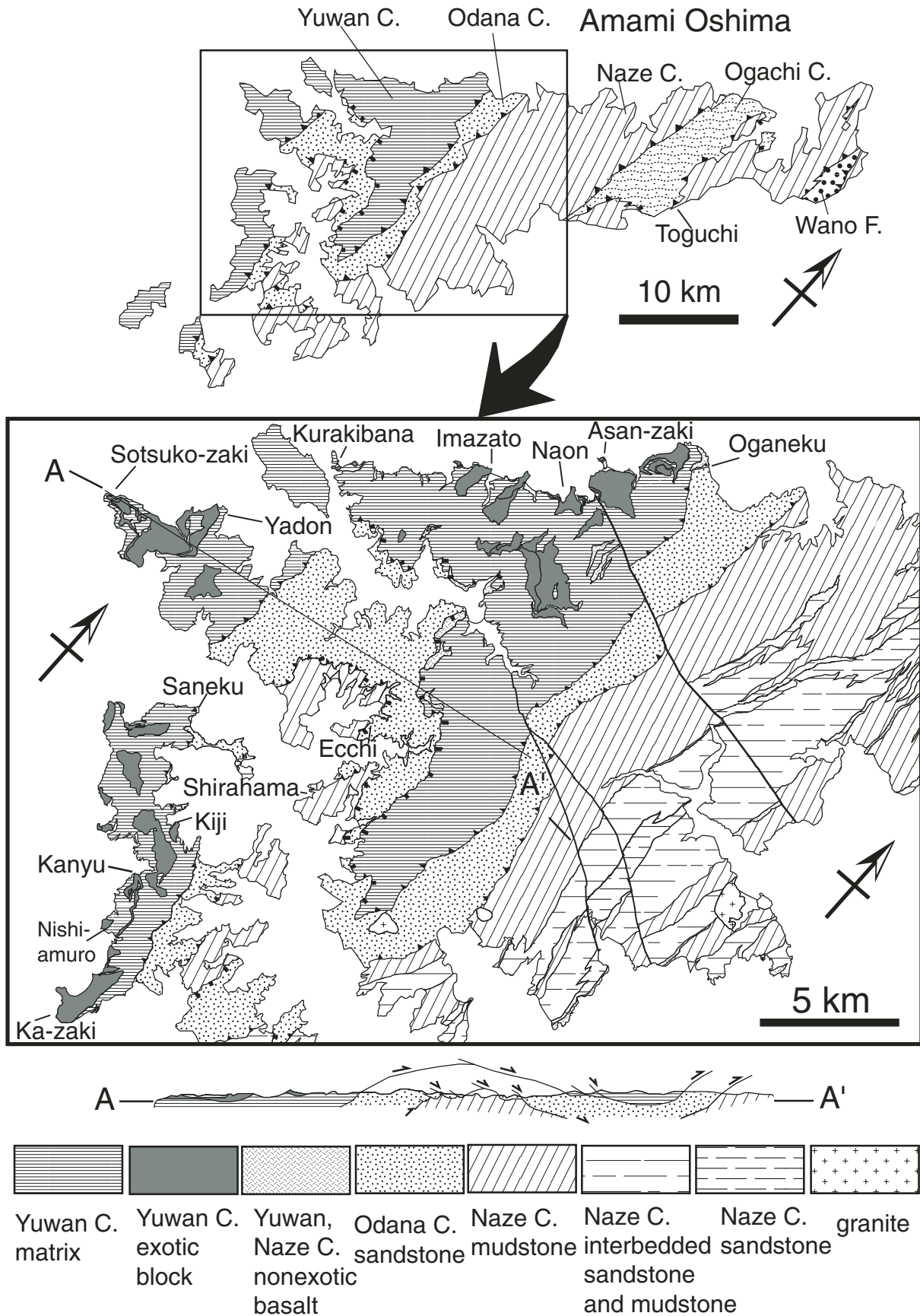


Figure 2. Geological map of the Yuwan complex (Osozawa, 1984). C—complex, F—formation.

consists of nonexotic basaltic lavas, hemipelagic mudstones, and terrigenous turbiditic sandstone, ascending in that order (Osozawa and Yoshida, 1997). Successions incorporating such nonexotic basalts resemble parts of an incomplete ophiolite, and hence they are referred to as “ophiolite” type (Xenophontos and Osozawa, 2004). The latter can thus be defined as basaltic lithologies that are characteristically overlain by, intercalated with, or partly intruded into hemipelagic (partly terrigenous turbiditic) mudstone, representing basaltic activity in a hemipelagic (partly terrigenous) depositional environment probably close to an ocean ridge-trench junction. The hemipelagic mudstone is siliceous and red to greenish in color, overlying or intercalated with the basalts. Contacts between siliceous mudstones and the basalts are depositional, while the basaltic dikes intrude the siliceous mudstone. Moreover, the hemipelagic mudstone itself is overlain by terrigenous turbidites of black mudstone and sandstone.

Given its volume, thickness, and distribution, the *mélange* component, however, constitutes a major part of the Yuwan complex. Block-in-matrix fabric tends to dominate in strata that are interlayered between the hemipelagic mudstones and turbidites and can be viewed in terms of a stratigraphic framework. The *mélange* matrix consists of black hemipelagic to terrigenous mudstones, associated in part with terrigenous sandstone, although the matrix is also interlayered with nonexotic basaltic lavas and crosscut by nonexotic dikes. The Yuwan *mélange* includes a substantial range of exotic inclusions with clast sizes varying from millimeter-scale to kilometer-sized blocks. The protolith ages, based mostly on radiolarians and fusulinids (Osozawa, 1984), vary with rock type as follows: basalts (Carboniferous to Triassic), cherts (Carboniferous to Permian), and siliceous, hemipelagic, black mudstones (Jurassic). The Jurassic mudstones were considered by Osozawa (1984) to be part of the *mélange* matrix, but an origin as unconsolidated exotic blocks in the *mélange* is now preferred.

The Odana complex consists of sandstone and mudstone and a relatively small proportion of exotic blocks, the latter of which are composed of basalt and hemipelagic mudstone characterized, in contrast to the Yuwan complex, by asymmetric shear fabric. The Naze complex consists of mudstone intercalated locally with basaltic lavas, hemipelagic mudstones, and silicic tuffs, and overlain by sandstone turbidites. Nonexotic basaltic intrusives are also observed. In the absence of asymmetric shear fabric, the widespread cleavage is exclusively due to pressure-solution, as observed in the Yuwan complex.

These three complexes are distributed within an apparent sequence of antiform and synform

structures, as indicated by dip directions of boundary faults and distribution pattern of the complexes (Fig. 2). However, the bedding and cleavage are not folded concordantly with mapable fold structures. The boundary of the eastern antiform limb is marked by composite listric normal faults, in contrast to the reverse faults associated with the western limb. The normal faulting has been interpreted as a consequence of gravitational slumping (Osozawa, 1984).

The Ogachi complex consists of bedded mudstones with intercalated sandstone lamina, representing distal turbidite and overlying proximal sandstone turbidite. Asymmetric folding is commonly observed to be associated with axial-planar pressure-solution cleavage resembling that in the other complexes. The Ogachi complex is bounded to the west by the central Naze complex, the boundary of which is marked by a brittle reverse fault, while its eastern boundary (with the underlying eastern Naze complex) is characterized by composite listric normal faults similar to those separating the Yuwan, Odana, and central Naze complexes in western Amami Oshima (Fig. 2).

The Wano Formation shows an upward-fining sequence of conglomerate, turbidite, and mudstone that takes the form of an overturned syncline (Ishida, 1969; Osozawa, 1984). Both eastern and western limits of the Wano Formation are marked by high-angle brittle fault contacts with the Naze complex. However, the conglomerates are interpreted to represent an original unconformity at the base of the Wano Formation. The conglomerate contains boulder-sized granite clasts, possibly derived from the Eocene intrusions, although the Turonian Ogachi complex also contains boulder-sized clasts of pre-Turonian granite.

GEOLOGIC FEATURES OF THE YUWAN COMPLEX

The Yuwan complex records several structural and depositional stages, suggesting that the block-in-matrix fabric is not the product of a single phase of deformation-induced shear, as is implied by the tectonic *mélange* hypothesis for the origin of this complex. Sedimentation stages are labeled Sd1 (sedimentary episode 1) and Sd2 (sedimentary episode 2), and deformation stages are referred to as D minus 1 (D_{-1}), D0, D1, and D2, respectively. Stratigraphic relationships suggest that these features are related as follows: as: Sd1 (Permian and Triassic), D_{-1} (Late Jurassic), Sd2 and D0 (Barremian), D1 (post-Barremian), and D2 (probably Eocene). Prograde metamorphism accompanying D_{-1} is M_{-1} , and D1 is M1, but D2 is associated with retrograde M2.

Sd1 is observed in the relatively large-scale exotic oceanic blocks that have lengthwise dimensions exceeding tens of centimeters. This applies to bedding and other sedimentary structures associated with chert layers, interbedded limestone and chert, and debris-flow deposits of variable clast size set in a finer-grained matrix of basalt, limestone, and chert.

D_{-1} is only recognized from structures within the exotic blocks, clasts, and fragments. This fabric (pressure-solution cleavage) is crosscut by an additional pressure-solution cleavage, D1. Older D_{-1} cleavage is also an axial-plane cleavage of D_{-1} asymmetrical cylindrical folds. No other asymmetric shear structures are observed. The D_{-1} cleavage is associated with recrystallized sericite mica belonging to M_{-1} . The combination of D_{-1} deformation and an M_{-1} thermal event demonstrates the existence of a separate older accretion event.

Sd2 contains primary lithologic layering of both terrigenous-sedimentary and igneous origin, and it includes the primary contacts of nonexotic basalt extrusives and intrusives of the Yuwan complex. Block-in-matrix fabric or *mélange* is consequently incorporated in Sd2. Interbedded sandstones and mudstones represent Sd2 trench-axial turbiditic deposits rather than *mélanges*. Nonexotic basaltic extrusive and intrusive contacts are also observed in Sd2 block-in-matrix fabric.

D0 represents a stage when deformation of soft sediments deposited on the inner-trench slope was triggered by slope instability, more or less contemporaneous with, or shortly postdating, Sd2 deposits. D0 structures include clastic dikes and slump folds and are overprinted by D1 cleavage.

D1 exhibits evidence of pressure-solution cleavage, including M1 sericite micas. The combination of D1 and M1 results from accretion of the Sd2 rock suite, overprinting all other suites, including turbidites, nonexotic basalts, muddy and sandy matrices, and exotic blocks. D1 cleavage, moreover, includes asymmetrical cylindrical folding and reverse faulting, but it lacks other asymmetric shear structures. Osozawa recently classified deformation stages with reference to the type of pressure-solution cleavage. This is simply labeled D1 for the accretionary and metamorphic complexes studied, and, in some cases, the cleavage is associated with asymmetric shear fabric (e.g., Osozawa et al., 2004; Schoonover and Osozawa, 2004; Osozawa, 2006). The absolute ages of D1 differ, of course, for these complexes, but they are useful for correlation and comparison of the structural features.

D2 folding was identified on the basis of folded D1 cleavage, while D2 faulting was identified from crosscutting D1 cleavage and the

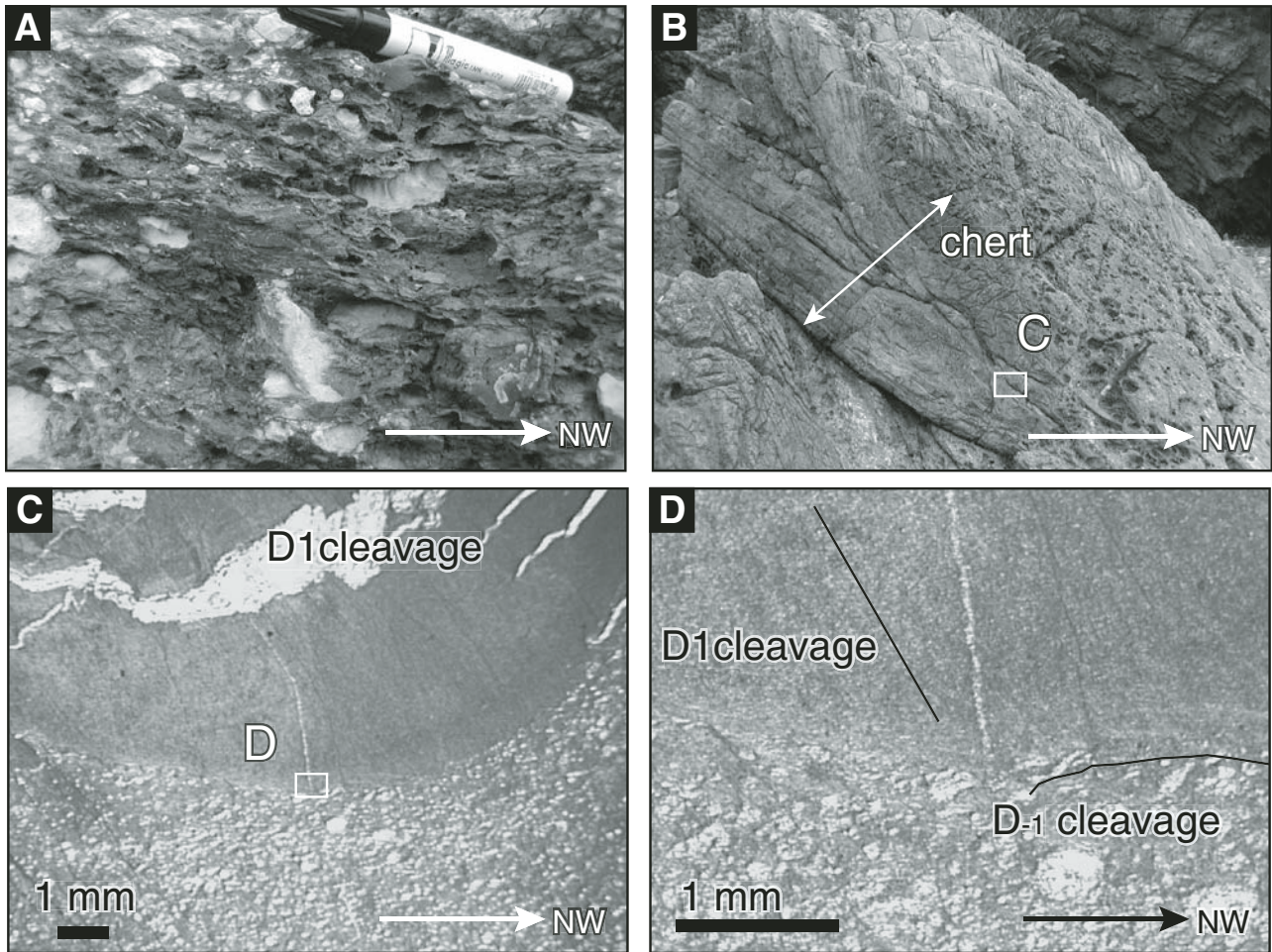


Figure 3. Sd1 debris flow, D₋₁ cleavages, and D1 fold at Naon coast. (A) Limestone and basalt clasts in limy and basaltic matrix. (B) Chert block folded with and mixed into matrix. (C) D1 axial plane cleavage in thin section. (D) D1 and older D₋₁, and M1 and older M₋₁ white micas in thin section.

existence of brittle gouge. D2 faults, both normal and reverse in character, mostly define the boundaries of the Amami Oshima complexes. They are not restricted to the Yuwan complex and are unrelated to the formation of its block-in-matrix fabric. The Eocene granitic intrusion, lacking evidence for, and postdating the D1 episode, probably predates the D2 episode.

Sd1: Internal Sedimentary Structure Restricted to Exotic Blocks

Exotic blocks of Permian and Triassic chert, often up to kilometer-scale in size, are interbedded with Sd1 argillitic partings. Such chert blocks are truncated by the Cretaceous muddy matrix and thereby show exotic provenance of the chert (Osozawa, 1984), along with Permian or Triassic basalts and associated oceanic debris-flow deposits. A single exotic block at the Ka-zaki cape section (Fig. 2) preserves the orig-

inal Permian to Triassic succession constituting these oceanic suites (Osozawa, 1986).

Three exotic kilometer-size blocks are tectonically emplaced and repeatedly exposed by D1 reverse faults and folds in the Naon coastal area (Fig. 2). The westernmost and tectonically highest block preserves a continuous Permian sequence in a road cut and nearby coastal section. In ascending order, lithologies in this section are debris-flow deposits, basalt extrusives, and interbedded cherts and limestone (Osozawa, 1986).

Clasts in the debris flow, ranging from a few centimeters to three meters in diameter, consist of basalt, chert, and limestone (Fig. 3A), while the matrix is made up of less than millimeter-sized fragments of basalt and limestone. These clasts are characteristically subangular to subrounded, poorly sorted, and matrix-supported (Fig. 3A). However, chert clasts, which also contain the late Permian radiolaria *Follicuculus scholasticus*, are lenticular and partly inter-

mingled with matrix at their margins (Fig. 3B), suggesting that the chert was semiconsolidated at the time of incorporation by the debris flow. Limestone clasts also contain the late Permian fusulina *Neoschwagerina margaritae*. Basaltic lavas, exposed exclusively in road cuts, are directly overlain by lenticular, reddish jasper interbedded with gray chert.

The total thickness of interbedded chert and limestone is 15 m, and each bedded layer consists of a composite layer of clastic limestone and overlying chert up to 1 m thick. The former consists of coarse-grained limestone with variably sized fragments of fusulina *Neoschwagerina* and other calcareous megafossils, with plagioclase and chlorite crystals at its base. The limestone becomes finer grained upward before giving way to the chert. Associated parallel- and cross-laminated structures in the finer-grained limestones confirm the limestone-chert assemblage to be turbiditic (Osozawa, 1986).

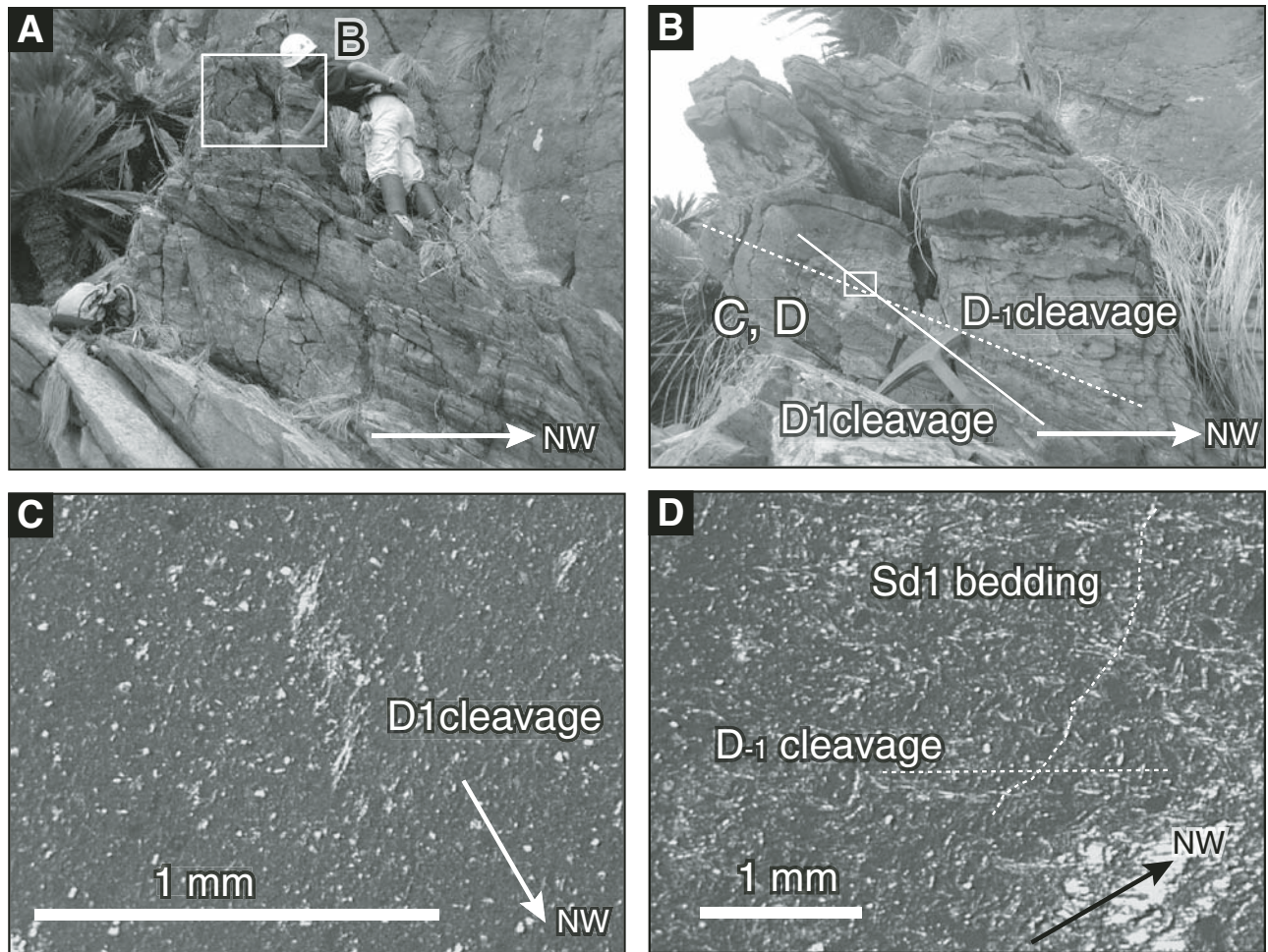


Figure 4. D_{-1} axial-planar cleavage fold and crosscutting D_1 cleavage at Asan-zaki Cape. (A) Bedded clastic limestone above the backpack and basaltic debris-flow deposit below. (B) D_{-1} asymmetric fold with axial-planar D_{-1} cleavage (dashed line, but unclear in this outcrop), overprinted by D_1 cleavage (solid line). (C) Trace fossil crosscut by D_1 cleavage, and associated M_1 white micas under cross nicols. (D) D_{-1} axial-planar cleavage, associated M_{-1} white micas, and crenulated S_{d1} bedding under crossed nicols.

As the product of an S_{d1} debris flow, the block-in-matrix fabric is clearly sedimentary in origin. The absence of accompanying terrigenous fragments (e.g., quartz) in the debris flow and turbidites indicates that they were deposited in an open-ocean setting, as expected, for example, on the flanks of a seamount during the Permian and Triassic (Osozawa, 1986). According to this interpretation, the limestone and basalt clasts could be derived, respectively, from a coral reef carapace and seamount basalt. The deposition of chert clasts accordingly represents material picked up by the debris flow from a seamount apron.

D_{-1} : Internal Deformation Structure Restricted to Exotic Blocks

Folded and faulted bedding is confined to exotic blocks of Permian and Triassic chert,

abraded by Cretaceous matrix, the latter of which provides additional evidence for an exotic provenance for the cherts (Osozawa, 1984). Two clear examples possessing D_{-1} older deformation structures are described next:

The first, at the Naon coast (Fig. 2), consists of an S_{d1} debris flow containing a relatively large (3-m-diameter) clast of bedded chert, which, together with the debris-flow matrix, is asymmetrically and cylindrically folded along a $N5^{\circ}E$ $8^{\circ}NE$ axis, with an axial plane of $N35^{\circ}E$ $55^{\circ}NW$ (Fig. 3B). The axial plane of this fold (Fig. 3C) coincides with the cleavage set observed in outcrop (Fig. 3B), but labeled D_1 (see D_1 section). Detailed thin section study shows that this D_1 pressure-solution cleavage overprints another pressure-solution cleavage, labeled D_{-1} , and the latter, parallel to the S_{d1} bedding of chert, is folded by a D_1 fold with

an axial plane of D_1 cleavage (Fig. 3D). D_{-1} cleavage is associated with the older white mica or sericite (0.02 mm long maximum; Fig. 3D), showing again a presence of M_{-1} metamorphism different from M_1 .

The second example is exposed at the Asan-zaki Cape section (Fig. 2), where exotic blocks ~100 m in scale consist of clastic limestone underlain by basalt-dominated debris-flow deposits, both of which are S_{d1} (Fig. 4A). The clastic limestone is bedded and folded asymmetrically and cylindrically (Fig. 4B). The axial plane is $N28^{\circ}E$ $32^{\circ}NW$, and the axial trend and plunge is $N22^{\circ}E$ $8^{\circ}SW$. However, strongly developed D_1 cleavage is observed in this outcrop (Fig. 4B), and it overprints the D_{-1} fold axial-plane obliquely and at a higher angle ($N25^{\circ}E$ $52^{\circ}NW$).

Petrographic study (Fig. 4C) shows that the D_1 cleavage represents a pressure-solution

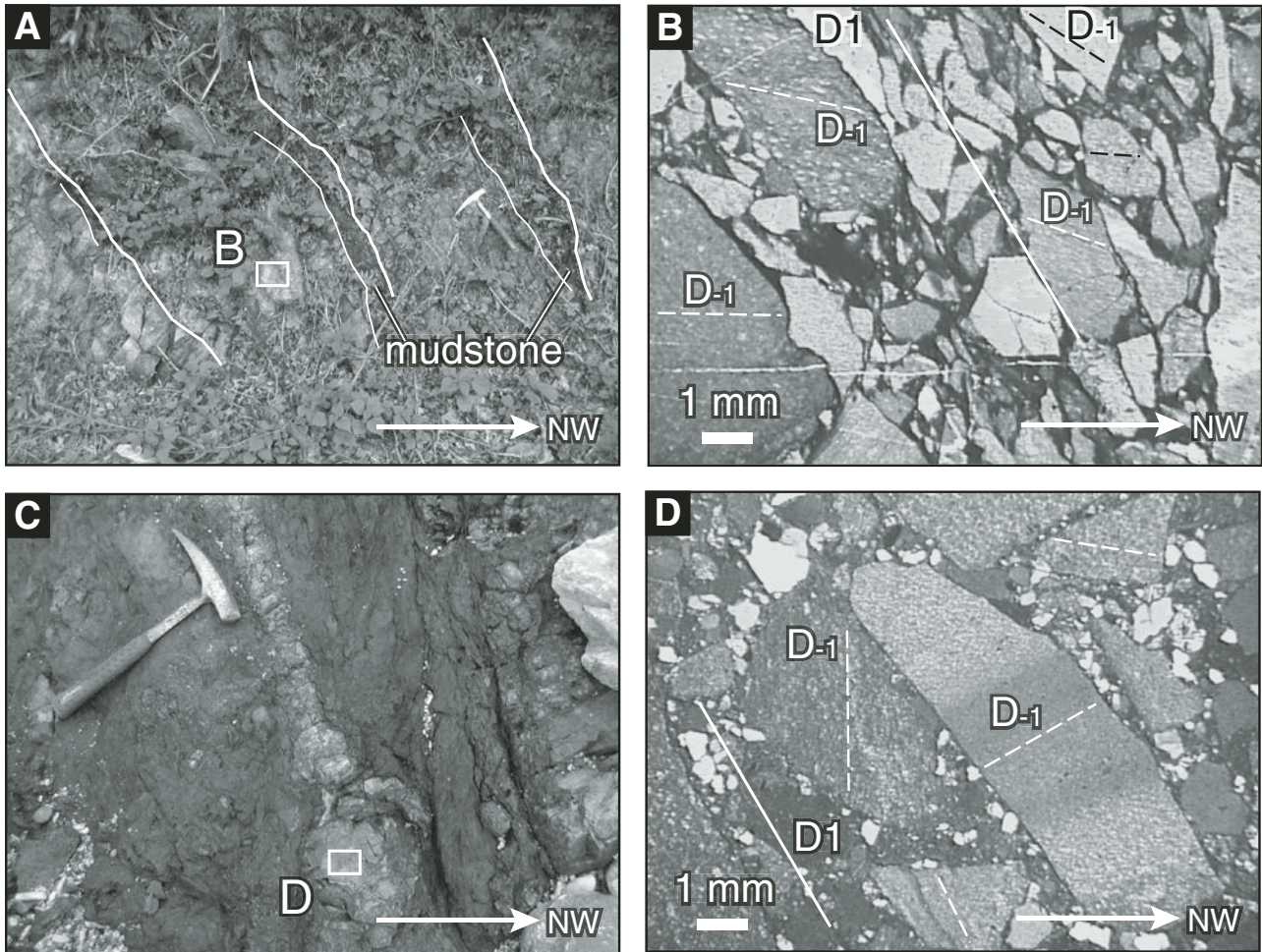


Figure 5. (A–B) Lithic sandstone at Naon coastal area. (A) Turbidite units. In each unit, sandstone consisting of chert fragments grades upward to mudstone. (B) D_{-1} cleavage within angular chert fragments, and D_1 cleavage at their margin, in thin section. (C–D) Pebbly mudstone at Kanyu coast. (C) Pebbly mudstone intercalated in muddy matrix. (D) D_{-1} cleavage within rock fragments, mostly chert. Fragmental margins are partly modified by D_1 cleavage.

cleavage with recrystallized sericite (maximum length: 0.03 mm), developed during the M1 episode. Sd1 basaltic fragments on this D_1 cleavage are rounded, indicating D_1 flattening strain. However, an additional set of D_{-1} pressure-solution cleavage planes at the fold-hinge is observed in thin section (Fig. 4D). This D_{-1} cleavage corresponds to the axial plane cleavage of the above D_{-1} asymmetric fold, and the Sd1 bedding consisting of basaltic fragments is crenulated by this D_{-1} cleavage (Fig. 4D). The latter is also accompanied by sericite (maximum length is 0.02 mm; Fig. 4D), and it records an M_{-1} prograde metamorphic event.

The D_{-1} fold is isoclinal (Fig. 4B), and the sense of shear appears to be normal, given the asymmetrical deformation of a tube-form trace fossil on the northwestern limb of the fold (Fig. 4C), contrary to the thrust shear sense

expected on the upper limb of an antiform. If we combine observations that the outer arc is a basalt-dominated debris-flow layer (Fig. 4A) and that the southeastern limb has normal Sd1 grading, the exotic block at the Asan-zaki Cape section must have been rotated by over 180° about a horizontal axis and inverted between the D_{-1} and D_1 events (i.e., during gravitational collapse and transportation on the inner-trench slope during Jurassic time, as discussed later), while the present northwestern limb was originally an overturned D_{-1} synform limb.

D_{-1} and Sd2: Internal Deformation Structure Restricted to Exotic Fragments and Clasts in Sd2 Debris Flow

Some exotic fragments and clasts included in Sd2 debris flows are undoubtedly of sedimen-

tary origin. Petrographic observations indicate significant distinct D_{-1} cleavage traces, and, in particular, these cleavage traces are confined to clasts where the cleavage is not continuous with that of the matrix. In this section, two types of debris-flow deposits that include such exotic fragments and clasts are described.

At several localities on the eastern Naon coast (Fig. 2), Cretaceous sandy and muddy matrix beneath the kilometer-scale exotic blocks intercalates with characteristic lithic sandstone layers. The latter make up composite layers up to 1 m in thickness of sandstone below and mudstone above (Fig. 5A). These sandstones characteristically consist of chert fragments (Fig. 5B) of probable Permian age, although small amounts of fragmented basalt and rip-up mudstone clasts are included. The chert fragments are characteristically angular, poorly sorted, and mostly matrix-

supported (Fig. 5B). Because of the observed grading and parallel lamination at the upper parts close to the mudstone transition (Fig. 5A), and partly in view of the associated inverse grading at its base, the sandstone layer is best explained as an Sd2 debris flow, and the combined sandstone-mudstone is best explained as a turbidite.

The turbidite was affected by D1 cleavage, which in outcrop crosscuts the Sd2 bedding at a high angle. In thin section, individual chert fragments show randomly oriented internal pressure-solution cleavage (Fig. 5B), while D1 pressure-solution cleavage is restricted to the contacts of each chert fragment (Fig. 5B). The cleavage confined within these exotic fragments is also referred to as D_{-1} , and the bedding is also referred to as Sd1.

Along the Kanyu coastal section (Fig. 2), blocks of bedded limestone, basalt, and chert are observed, along with conglomerate (pebbly mudstone) layers intercalated in the matrix (Fig. 5C). This type of conglomerate is also exposed along the Imazato and Nishiamuro coasts (Fig. 2). The conglomerate clasts, which include also chert, basalt, limestone, and a minor siliceous mudstone, are rounded to angular, poorly sorted, matrix-supported, and as a whole show normal grading (Fig. 5C), indicating a debris-flow origin. The clasts invariably show unique, randomly oriented internal cleavage and bedding (Fig. 5D), while D1 pressure-solution cleavage is again restricted to the contacts of each cherty fragment (Fig. 5D). The cleavage within the chert and siliceous mudstone fragments is therefore labeled D_{-1} .

D_{-1} strain at the Kanyu locality can be determined on the basis of deformed radiolarians in a single siliceous mudstone fragment. The strain field is of oblate type, similar in geometry to that of D1 (see D1 strain section). Sericite, observed along D_{-1} cleavage in several siliceous mudstone fragments, shows older-phase, prograde M_{-1} metamorphism. Measured b-cell dimensions of white mica indicate that the metamorphism is also medium P - T type, not the high P - T type expected at a subduction zone setting (see M1 section).

Sd2: Block-in-Matrix Sedimentary Structure

Other than the lithic sandstones and pebbly mudstones, muddy matrix-dominant block-in-matrix fabric is widespread in other parts of the Yuwan complex.

In the western part of the Naon coastal section (Fig. 2), the muddy, mostly siliceous matrix is Cretaceous in age, according to the types of radiolarian present. These rocks contain isolated and angular ten-centimeter-scale clasts of exotic bedded limestone and chert, showing Sd1 inter-

nal sedimentary structure (Fig. 6A), that rest on the kilometer-scale exotic blocks. The matrix, however, also contains millimeter-sized basalt fragments in addition to limestone and chert. All inclusions are characteristically subangular to subrounded, poorly sorted, and matrix-supported. Together, however, they constitute weakly developed lithologic and size laminations, and they appear to represent discrete debris-flow units.

Symmetric D1 pressure-solution cleavage also overprints the clasts as well as matrix (Fig. 6B). However, exceptionally rare asymmetric pressure shadows (Fig. 6B) are observed near a D1 reverse fault, which cuts an isolated clast (Fig. 6A).

Outcrop-scale exotic clasts are thus interpreted as inclusions in Sd2 debris flows. Also, kilometer-sized exotic blocks observed, for example, at the Naon coastal and Ka-zaki Cape sections (Fig. 2) can be explained as very large inclusions within the debris flows (cf. Lucente and Pini, 2003). However, such kilometer-sized blocks may be more reasonably explained in terms of submarine slides or slumps rather than mass flows (Osozawa, 1984).

The dominant sequences of bedded sandstone and mudstone represent turbiditic trench fill deposits, and they may have originally occupied the highest stratigraphic position in the Yuwan complex. This may also have been the case at the Asan-zaki Cape section (Fig. 2), apart from the exotic blocks, in which a fragment of basalt, in addition to fragments of quartz and detrital white mica, is recognized in thin section. At the Kurakibana Cape and Saneku coastal sections (Fig. 2), for example, exotic chert blocks appear sporadically within such turbidites. Submarine mass wasting is thus a reasonable mechanism for transporting both detrital-terrestrial and exotic oceanic clasts.

Sd2: Nonexotic Basaltic Extrusive and Intrusive Structures

Other than exotic basaltic rocks, the Yuwan complex is characterized by nonexotic basaltic extrusions and intrusions of Barremian age emplaced with coeval mudstones and sandstones. Basaltic activity in the Shimanto zone, including the Naze complex, Amami Oshima, is characteristic of that expected at a trench-trench-ridge triple junction, assuming its diachronous migration along the Ryukyu and SW Japan arcs (Osozawa and Yoshida, 1997). Nonexotic basalts in the Yuwan complex represent the products of previous magmatic activity at an earlier trench-ridge junction.

The nonexotic extrusives, including pillow lavas, tend to occupy the lowermost horizons of the Yuwan complex, distributed mostly along

the D2 faulted contact with the underlying Odana complex. Similar lavas are also exposed along the Oganeku coast (Fig. 2), where they are overlain by Barremian red siliceous mudstone (Osozawa, 1984; Osozawa and Yoshida, 1997). The mudstones are bedded but contain plagioclase and quartz fragments, and they show lower silica contents $< \sim 90\%$ (cf. the exotic bedded cherts; Osozawa, 1984). The mudstones grade upward from red- to green-colored to black, above which, the black mudstone is associated with sandstone layers and exotic blocks. The red- and green-colored mudstones are affected by SE-vergent D1 axial-planar cleavage and folding only (Osozawa, 1984), contrasting with randomly oriented (Osozawa, 1984) D_{-1} folding in exotic chert clasts. Nonexotic basaltic intrusions also appear in middle and upper horizons of the Yuwan complex, and also in exotic blocks and their matrices (Osozawa, 1984).

In the Naon coastal section (Fig. 2), the lowermost exotic block forms a synform, the southeastern limb of which consists of basaltic lava overlain by chert. The contact with the overlying middle block is a D1 reverse fault. The hanging wall of chert is associated with SE-vergent D1 asymmetric folds (part of an antiform), and the footwall basalt and chert strike $N15^{\circ}E$ and dip $30^{\circ}SE$ (part of a synform). While jasper is intercalated between this exotic basaltic lava and chert, two (nonexotic) basaltic dikes intrude the succession along planes of $N70^{\circ}E$ $85^{\circ}NW$ and $N80^{\circ}E$ $85^{\circ}NW$ (Figs. 7A and 7B). Chilled margins on the basaltic dikes are in turn overprinted by D1 pressure-solution cleavage (Figs. 7C and 7D). Sericite developed along the D1 cleavage, and pumpellyite developed in the host dike, both of which appear to reflect M1 metamorphism.

Intrusions of camptonite, an alkali basalt variant (Osozawa, 1984; Kanisawa et al., 1983; Osozawa and Yoshida, 1997), are also exposed in a road cut close to the Naon coast (Fig. 2). D1 cleavage is again recognized in chilled glass margins in these intrusions, suggesting that they represent pre-D1 nonexotic intrusives in the Yuwan complex.

Another basaltic rock of alkaline affinity, spessartite, intrudes the Yuwan complex and, like camptonite, may indicate a "hotspot" origin (Osozawa and Yoshida, 1997). In contrast, the spessartite crosscuts muddy matrix, showing strong D1 cleavage while showing no signs of cleavage within itself. Thus, the spessartite is a post-D1 (postaccretion) intrusion, and it does not represent a "nonexotic" basalt component in the Yuwan complex. Spessartite intruding bedded sandstones and mudstones of the Odana complex (Takeuchi, 1993) appears to be directly analogous.

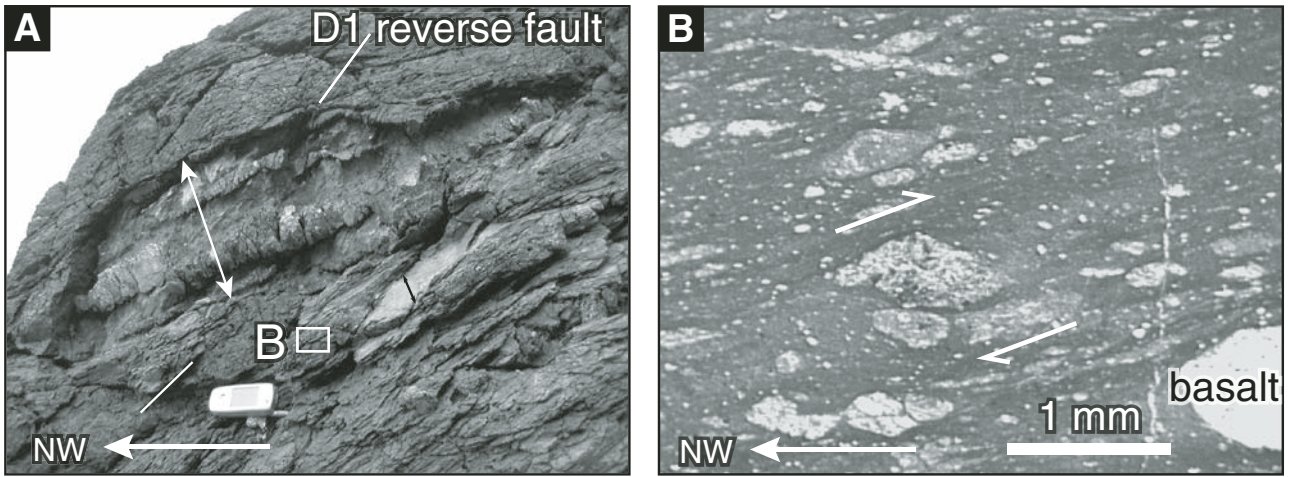


Figure 6. An exotic clast of bedded limestone and chert at Naon coast. (A) Reverse fault cutting both the exotic clast and matrix. Other exotic chert fragments are visible. (B) Asymmetric pressure shadow close to reverse fault, in thin section.

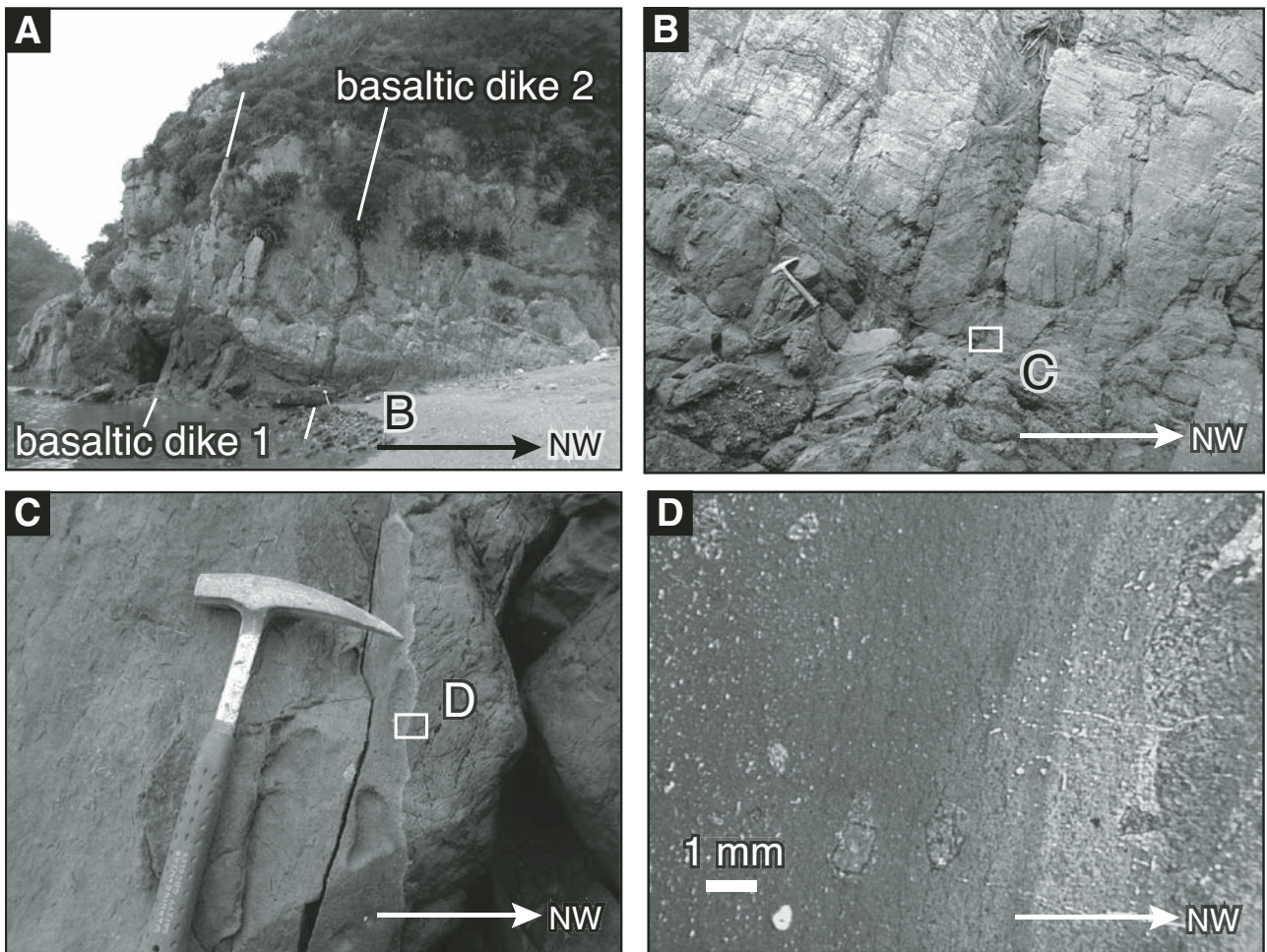


Figure 7. Nonexotic basaltic dikes at Naon coast. (A) Basaltic dikes 1 and 2 intruded into a succession of pillow basalt below and chert above. (B) Jaspers are intercalated near the top of basaltic lava and intruded by basaltic dike 2. (C) Western chilled margin of basaltic dike 2. (D) D1 pressure-solution cleavages in the chilled margin, under thin section.

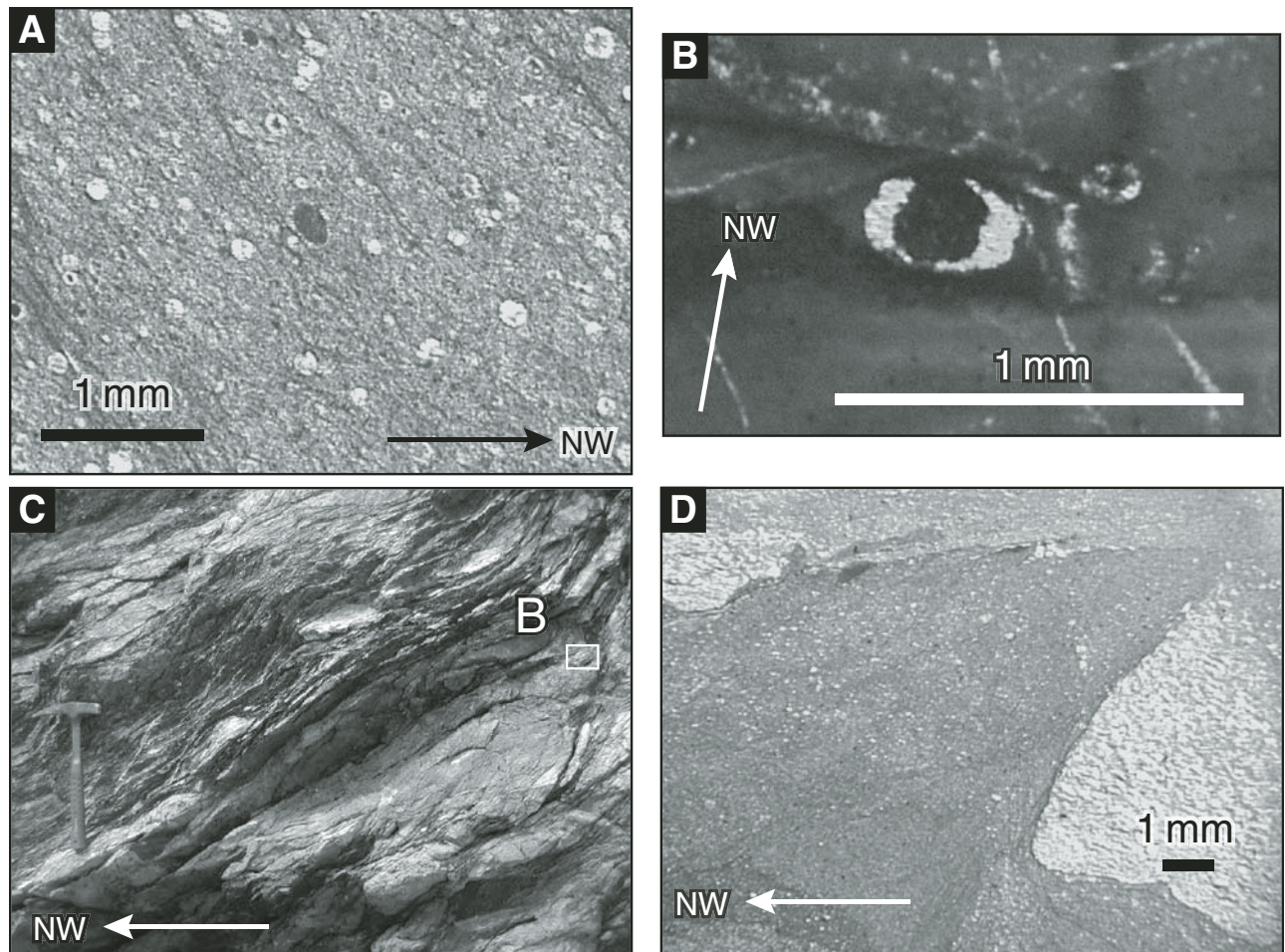


Figure 8. D1 structures at Naon coast, but part B is from Sotsuko-zaki Cape (Fig. 2). (A) Pressure-solution cleavage. Radiolarians are deformed or truncated by pressure solution. (B) Symmetric pressure fringe. (C) D1 asymmetric fold. (D) D1 axial-plane and pressure-solution cleavage, thin section view.

A basaltic dike is also observed in the Odana complex in the Oganeku coastal section (Fig. 2), close to the D2 brittle fault contact with the Yuwan complex. The chilled margin of the dike cross-cuts the cleavages, indicating that it is a post-D1 and probably post-D2 intrusion, i.e., more or less coeval with Eocene granitic intrusives rather than nonexotic basalts in the Yuwan complex.

D0: Matrix Soft-Sediment Deformation

Sd2 debris flow and sliding accompanied soft-sediment deformation, indicating that the matrix was not consolidated when exotic blocks were emplaced and incorporated to form block-in-matrix fabric. The most unusual phenomenon observed was a mud dike intruded into exotic basaltic blocks at Kiji and elsewhere (Fig. 2; Osozawa, 1984).

Radiolarian-rich layers in siliceous mudstone represent clastic dike intrusions at the western-

most end of the Naon coastal section (Fig. 2). These dikes, ranging in width from millimeters to centimeters in scale, show similar D1 trends to those of pressure-solution cleavages, although petrographic study shows them to be clearly overprinted. The intrusive event is thus referred to as D0, when the original platy fabric was formed by presumable grain-boundary sliding (cf. Schoonover and Osozawa, 2004, p. 227).

Turbiditic arkosic sandstones, further overlying the siliceous mudstone, show recumbent folding with an axial plane that is highly oblique to the D1 cleavage overprint. This indicates SE-vergent D0 slump folding, consistent with a trench-inner-slope provenance (Osozawa, 1984).

D1: Deformation Structure both on Matrix and Exotic Blocks

Block-in-matrix fabrics, including exotic blocks and other Sd2 fabrics, invariably involve

accretionary tectonic deformation at depth, as already described.

Pressure-solution cleavage attributed to D1 deformation (Fig. 8A) is evident in siliceous mudstones in the westernmost part of the Naon coast (Fig. 2), and it is ubiquitous in other Japanese accretionary complexes. The siliceous mudstone is intercalated with thin (millimeters-thick) radiolarian layers, from which the D0 clastic dike is derived. The siliceous mudstone was affected by an episode of pressure-solution cleavage, clearly evidenced by the solution of radiolarian tests, detrital quartz, and muscovite grains (Fig. 8A); the cleavage is marked partly by the presence of sericite, representing metamorphic event M1, and partly by alternating, opaque dusty layers. There is no asymmetric shear fabric associated with this cleavage (Fig. 8A). Pressure shadows and fringes are symmetric (Fig. 8B), with an exception close to the D1 reverse fault (Fig. 6B). Moreover, finite

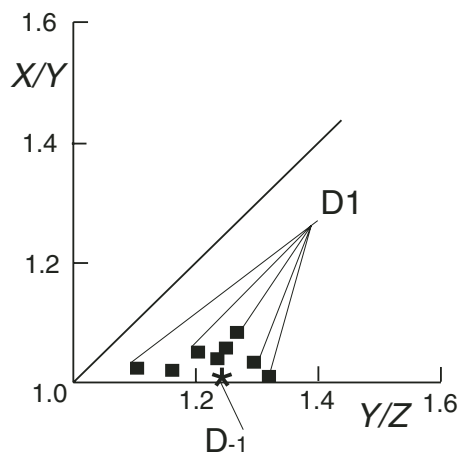


Figure 9. Flinn diagram. Eight plots are from mudstone (D1), and one plot is from a siliceous mudstone fragment at Kanyu coast (D₋₁).

strain determined from radiolarian morphologies records nearly pure flattening (see following), which is inconsistent with simple shear constriction. Together these observations indicate that noncoaxial strain, indicative of shear, was not present during D1 cleavage formation at the brittle-ductile transition stage.

The cleavage strikes NE along this coastal section, dipping moderately to the NW, equivalent to D1 cleavage in the Yuwan complex. Asymmetric folding is commonly observed in the siliceous mudstone, the axial plane of which coincides with the pressure-solution cleavage (Figs. 8C and 8D). Accordingly, the axial-planar cleavage ascribes this folding to the D1 deformation phase. Reverse faulting is also common at the overturned limb of asymmetric folds (Figs. 6A, 8C, and 8D). The fault is associated with opaque minerals and quartz veins rather than gouge.

D1 Strain Type

D1 strain was determined with a view to testing and quantifying the extent of symmetric deformation. Oblate type strain, where distinguishable, indicates no stretching lineation and no asymmetric shear. The departure from the originally spheroidal form of radiolaria provides a useful method of analyzing the effects of strain, as long as radiolaria demonstrably affected by pressure solution are avoided. A total of nine radiolarian mudstone samples was examined, following the method of Kimura and Mukai (1991) and Osozawa et al. (2004). Sections were cut relative to strike because of the lack of clear stretching lineation on the cleavage. Two orthogonal sections were cut perpendicular to the D1 cleavage: one parallel to and the

other perpendicular to the strike. The lengths of long and short axes were then measured for over 20 deformed radiolarians in each section. Their approximated lines of $X = aZ$ and $Y = bZ$ (where $a > 1$, $b > 1$, and $a > b$) were established, and a Flinn diagram was created (Flinn, 1962; Fig. 9).

The D₋₁ data plotted for the Kanyu coast section are for the radiolarian mudstone fragment, already mentioned. Although data were only obtained for this sample, the D₋₁ and eight other D1 strain-ellipsoids are all of flattening type (Fig. 9), suggesting that asymmetric shear deformation would not be expected for either D₋₁ or D1 and that these pressure-solution cleavages correspond to the observed slaty cleavages.

Oblate type strain has been commonly observed in Japanese accretionary complexes (Toriumi and Teruya, 1988; Kimura and Mukai, 1991; Osozawa et al., 2004), but it differs from the prolate type associated with constrictional shearing along stretching lineations as reported from the Shimanto zone of Kyushu and Okinawa (Needham, 1987; Toriumi and Teruya, 1988; Schoonover and Osozawa, 2004).

M1 Metamorphism

Metamorphic minerals in both exotic and nonexotic basalts include prehnite, pumpellyite, and (rare) actinolite, probably reflecting medium *P-T* metamorphism. However, such mineral assemblages in such low-grade rocks are comparatively insensitive to pressure and temperature, and also metamorphic phases associated with ocean-floor metamorphism are commonly the same as those that form during burial metamorphism. In addition, the exotic basalts showed more extreme oxidation and albitization histories than the nonexotic basalts (Osozawa, 1984; Osozawa and Yoshida, 1997), perhaps reflecting more than a single episode of prograde M₋₁ and M1 metamorphism, but it was hard to distinguish between M₋₁ (D₋₁) and M1 (D1) in the mildly deformed basalts. On the other hand, M₋₁ and M1 metamorphic minerals in pelitic rocks are distinguishable, syntectonic with D₋₁ or D1, and absent from ocean-floor metamorphic assemblages.

Substitution of Tschermak's molecule in phengite and muscovite in pelitic rocks is both temperature- and pressure-sensitive, especially when the latter barometric estimates are derived from data for *b*-axis lattice-constants (Guidotti et al., 1989), which may be obtained using the relationship (Guidotti et al., 1989), e.g., $b = 8.9931 + 0.0440 (\text{Mg} + \text{Fe})$ on the basis of Mg, Fe, and Al contents (obtained using an energy-dispersive spectrometer [EDS] attached to a scanning electron microscope). Cumulative frequency curves generated from b-cell dimen-

sions of sericite were used as a basis for geobarometric estimates (Sassi and Scolari, 1974). The resulting curves show one sample of M₋₁ (mentioned previously) and five M1 samples equilibrated under medium *P-T* metamorphic conditions (e.g., temperatures of ~250 °C and pressures of ~0.25 GPa; Fig. 10).

Estimating b-cell parameters can also be accomplished by means of X-ray diffraction (XRD) studies. Using this method, medium *P-T* conditions based on cumulative frequency curves were also obtained, and pressures for equivalent temperatures were a little lower than those derived from EDS data but still essentially corroborated the conditions inferred for the Yuwan complex as a whole (Fig. 10).

Values of illite crystallinity (also referred to as the Kübler Index) were also obtained using XRD, and they served as a basis for estimating geothermal conditions in mudstones of sub-greenschist to greenschist metamorphic facies (Kübler, 1968; Underwood et al., 1993). Illite crystallinity values (0.21–0.31) were obtained only for M1 conditions, corresponding to the epizone and high anchizone of Kübler (1968).

Although relatively high *P-T* ratios (e.g., up to 350 °C and 0.6 GPa for the low-grade Sambagawa metamorphic rocks) at relatively low geothermal gradients are generally expected in subduction zone settings, our estimates of *P-T* metamorphic conditions based on EDS and XRD data are not unexpected for accretionary complexes proximal to a (thermally anomalous) setting such as a ridge-trench intersection (e.g., Osozawa et al., 2004), which is the genetic setting inferred for the Yuwan complex (see previous discussion).

D2 Brittle Structure

Despite the common observation of D2 deformation effects in the Yuwan complex, they were not fully described by Osozawa (1984) except for fault contacts between accretionary complexes. In this section, such D2 structures are described more comprehensively.

Out-of sequence thrusting (Fig. 11A), corresponding to D2 faulting, was probably first reported from the Shimanto zone of Shikoku (Onishi and Kimura, 1995). However, the apparent lack of distinction may have been misleading between composite structures of D2 overlapping D1 and the true D1 Riedel shear. Careful petrographic study is thus required for identification of asymmetric shear structures in mélange lithologies (e.g., Osozawa et al., 2004; Schoonover and Osozawa, 2004).

Cylindrical D2 folds have deformed and bent the D1 cleavage (both are then distinct), along a NE-SW axis and mostly NW-dipping axial

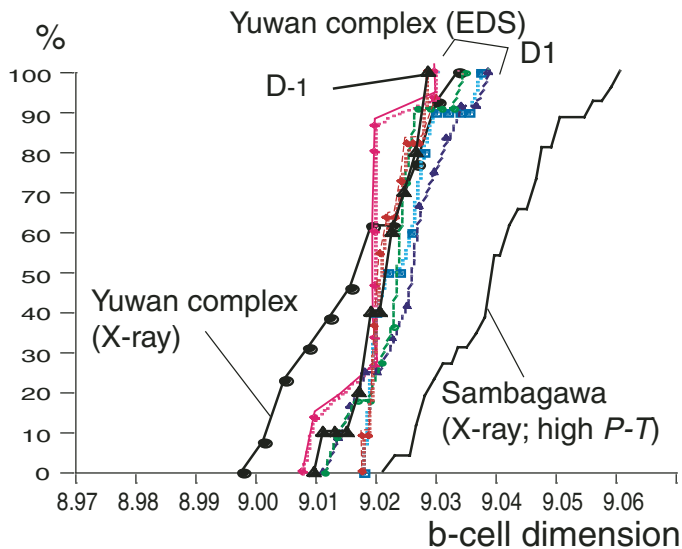


Figure 10. Cumulative frequency curve of b-cell dimensions of white mica. High pressure-temperature (P - T) curve is referenced by the Sambagawa curve (Schoonover and Osozawa, 2004). EDS—energy-dispersive spectrometry.

An example of normal faulting between the Ogachi and Naze complexes is evidenced by the asymmetric distribution of sigmoidal quartz veins exposed in the Toguchi coastal section (Fig. 2).

The D2 normal faulting is probably related to exhumation of the Naze complex, which was metamorphosed at a relatively higher grade than the footwall complexes, and can be compared to exhumation of the corresponding Nago metamorphic rocks, Okinawa, in the Shimanto zone (Schoonover and Osozawa, 2004; Fig. 1). According to Schoonover and Osozawa (2004), the principal factor causing D2 deformation and M2 metamorphism is that of mid-oceanic ridge subduction during Eocene time.

DISCUSSION: SEDIMENTARY VERSUS TECTONIC MÉLANGE FORMATION; AN INDICATION OF MULTIPHASE ACCRETION AND RECYCLING

It is now widely accepted that extensive asymmetric-shear fabric is a defining characteristic of tectonic mélanges (Onishi and Kimura, 1995). However, the Yuwan complex completely lacks such an asymmetric fabric both in D1 and D₋₁ and, accordingly, the defining features ascribed to tectonic mélanges. Thus, the formation of asymmetric and the formation of block-in-matrix fabrics are considered to represent two independent processes, supported additionally by the intense shear fabric observed in the Okinawa Nago complex, along with the absence of block-in-matrix fabric (Schoonover and Osozawa, 2004). The lack of dependence is also suggested by the unlikelihood that D1 cleavage has given rise to the extensive shear-related displacement onto Sd1, especially with regard to the nonexotic basaltic intrusions. Instead, Sd1 and Sd2 block-in-matrix fabric is actually observed. Moreover, for tectonic mélange generation, all block and matrix contacts would be required to

plane (Fig. 11B). The axial plane reflects mild pressure-solution cleavage but lacks evidence of M2 sericite recrystallization (Fig. 11C), indicating, therefore, that M2 is a retrograde phase.

D2 faults are brittle and associated with gouge, and observed striations correspond to both reverse and normal faulting. D2 faults strike NE-SW, and most reverse faults dip NW, whereas most normal faults dip SE. These faults often accompany SE-directed D2 parasitic folds.

The boundaries between the different complexes are marked by both normal and reverse faults (see Osozawa, 1984, and figures therein). A good example of reverse faulting is observed on the Shirahama coast (Fig. 2), where sand-

stone and mudstone of the Odana complex rest on mudstone associated with silicic tuff of the Naze complex. This fault has 1.5 m gouge and NW-plunging striation. The asymmetric structure observed in foliated gouge indicates SE-directed thrust-sense shear.

Examples of composite reverse and normal faults are observed in the Ecchi coastal section (Fig. 2). These faults show a composite set of concave-upward configured normal faults and reverse faults. The D1 cleavage of the Naze complex is cut and that of the Odana complex is bent by these faults. However, the fault surfaces are sometimes irregular, probably indicating the effects of D2 gravity sliding (Osozawa, 1984).

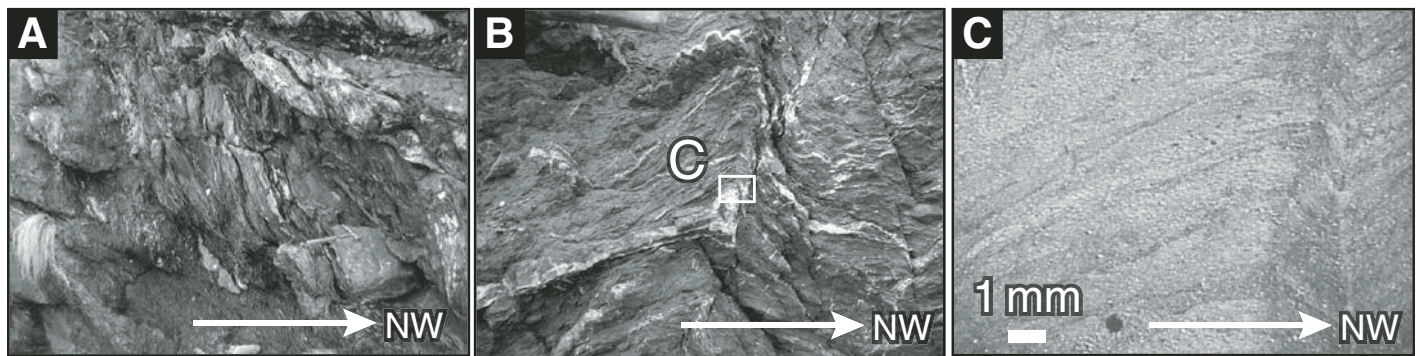


Figure 11. D2 structures at Asan-zaki cape (A) and Yadon coast (B-C; Fig. 2). (A) D2 out-of sequence thrust (apparent D1 Riedel shear). (B) D2 fold at coastal outcrop. (C) D1 bent kink fold in thin section.

exhibit shear planes, despite the preservation of original depositional contacts.

Unconsolidated matrix is evidenced by D0 clastic diking and slump folding. The generation of floating blocks in muddy matrixes by tectonic activity would be equivalent to transfer of consolidated exotic blocks into such unconsolidated matrix by pervasive and coeval shearing, requiring the (unlikely) transmission of shear force into soft sediments. Moreover, the graphic model for tectonic mélangé formation proposed by Wakita (2000) cannot be reconciled with the original (inferred) ocean crustal stratigraphy.

In summary, the observed field relationships described in this paper suggest that the block-in-matrix fabric of the Yuwan complex is a sedimentary fabric that formed by debris-flow deposition. Strongly supporting evidence for this contention includes the notion that exotic fragments may be taken simply to represent sedimentary detritus, including pre-existing D_{-1} pressure-solution cleavage effects offering a record of older tectonic event. Sd1 oceanic debris-flow deposits, and Sd2 chert clastics and pebbly mudstone at Naon and Kanyu are additional clear evidences of sedimentary origin of mélangé.

The Yuwan complex is thus believed to record multiple sedimentary and tectonic events, the relative and absolute chronology and geometric and spatial relationships of which are demonstrated in the present study. This scenario is in contrast to a single-phase or continuous shearing event or episode of the type hitherto assumed

to be responsible for the generation of tectonic mélanges (e.g., Onishi and Kimura, 1995).

The oldest record preserved in the Yuwan complex is the Sd1 block-in-matrix fabric, representing a debris flow where material of oceanic provenance is only mixed on slopes of an intraplate volcanic edifice in response to the gravitational collapse of the latter. This model, in contrast to the notion that Sd2 fabric results from additional mixing of terrigenous suites along inner-trench slopes, was first proposed by Osozawa (1986), and we contend it is further supported by the present study.

The second record is D_{-1} pressure-solution axial-planar cleavage lacking asymmetric shear fabric overlapping Sd1 block-in-matrix fabric, and M_{-1} medium P - T metamorphism occurring as a result of the D_{-1} pressure-solution. The mode and combination of D_{-1} deformation and an M_{-1} thermal event demonstrate the existence of a separate, older accretion event than that interpreted for the Cretaceous, wherein Permian and Triassic oceanic products were recycled and mixed within the (probably) Jurassic accretionary prism, which may be inferred from Jurassic exotic hemipelagic mudstones in the Yuwan complex. According to this model, Sd2 represents a depositional event at a trench axis, where an existing accreted oceanic suite was incorporated by debris flows and mixed with a terrigenous matrix. Sd2 accompanied D0 soft-sediment deformation at the trench-inner slope, undergoing gravitational collapse and activating additional debris flow. We con-

jecture that the already accreted, D_{-1} -deformed, and M_{-1} -metamorphosed oceanic suite was then exhumed, thereby triggering a large-scale debris flow. Intercalation of mélangé between hemipelagic and terrigenous units is the inevitable consequence.

D1 deformation and M1 metamorphic conditions appear to be unique to active mobile zones, and oceanic and terrigenous rock assemblages are also exclusive to an accretionary prism setting. The Sd2 relationships of nonexotic basalts, especially where these are intrusive, are abnormal, except in the setting of an accretionary prism influenced by a ridge-trench interaction. The inferred medium P - T metamorphic conditions and D2 orogenic events are consistent with the notion of a ridge-trench interaction, as proposed by Osozawa et al. (2004) and Schoonover and Osozawa (2004). According to this model, the oceanic suite, having recorded D_{-1} and M_{-1} episodes, was subsequently accreted during Barremian time (Fig. 12). The accretion process probably involved off-scraping as characterized by present D1 symmetric flattening, rather than underplating, which is characterized by asymmetric constriction and believed to occur at significant depth. Subsequent underplating would thus be unrelated to the tectonic mélangé process (cf. Hashimoto and Kimura, 1999).

In summary, several lines of evidence suggest that oceanic materials, as well as older terrigenous materials, are recycled mostly by sedimentary processes within an accretionary prism (Fig. 12; Osozawa, 2006). Although recycling

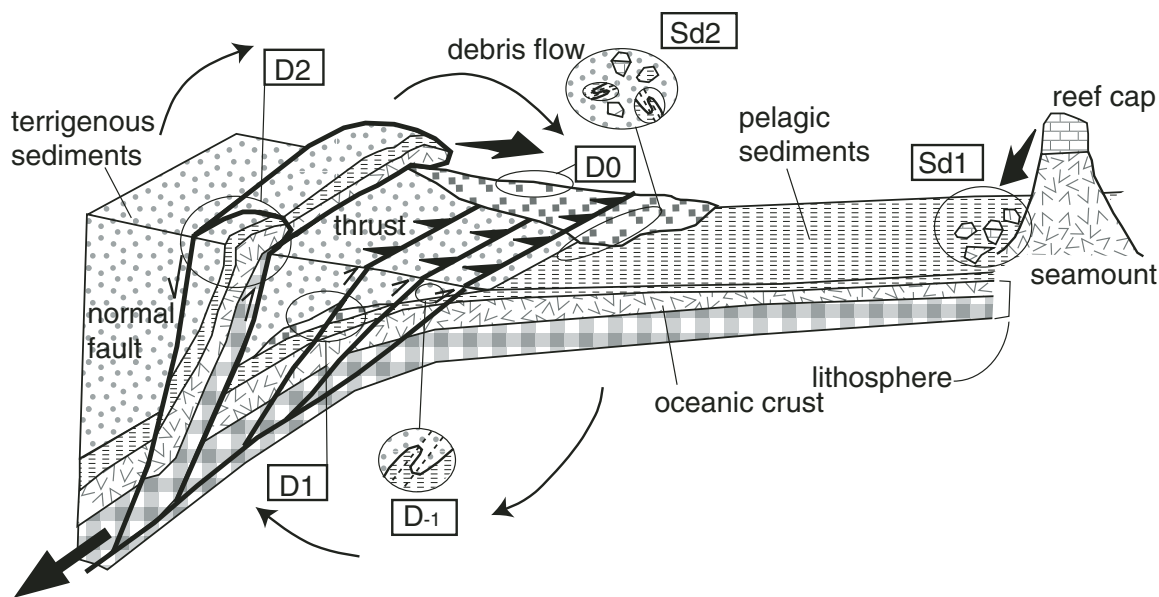


Figure 12. Recycling model of oceanic and terrigenous materials, followed by labeled deformation phases.

under high P - T conditions was reported in the Franciscan Complex by Cowan and Page (1975), we offer here, for the first time, convincing evidence of such recycling in the ancient Ryukyu arc-trench system, and our recent studies of Japanese accretionary complexes (e.g., Osozawa, 2006) suggest that the term “tectonic mélange” should be applied with caution.

CONCLUSION

The Yuwan complex, in the SW Japanese Ryukyu arc, exhibits two types of Sd1 and Sd2 block-in-matrix structures, both of which show characteristics of sedimentary debris flow. The D1 symmetric deformation effects were overprinted on these block-in-matrices, although the lack of shearing precludes transportation of the oceanic blocks into the matrix, and thus discards the tectonic mélange hypothesis. All the Sd1, Sd2, including nonexotic relationships of basalt, D₁, and D0 structures are well preserved, avoiding the tectonic disturbance supposed in a tectonic mélange. Our study is also the first to record a clear D₁ deformational episode in an accretionary complex, indicating that the oceanic suite was almost certainly recycled in a subduction zone setting.

ACKNOWLEDGMENTS

We appreciate constructive reviews by Yildirim Dilek and Brendan Murphy (editors), John Wakabayashi (associate editor), Terry Pavlis, and one anonymous reviewer, and encouragement from Hiroyuki Otuka at Kagoshima University. Accommodation and support for the second author was kindly provided by Ikuya Hajime, Tokio Nakae, and the Yuwan Youth Committee. Hitoshi Hasegawa, Kazuyuki Yamamoto, Takayuki Sakai, Tomoki Ishii, and Yoichi Usui are thanked for help with analyses using energy-dispersive spectrometry (EDS) and X-ray diffraction (XRD) methods. The third author gratefully acknowledges the hospitality and excellent working conditions afforded by Tohoku University during two months spent as Distinguished Visiting Professor.

REFERENCES CITED

Brandon, M.T., 1989, Deformational styles in a sequence of olistostromal mélanges, Pacific Rim Complex, western Vancouver Island, Canada: *Geological Society of America Bulletin*, v. 101, p. 1520–1542, doi: 10.1130/0016-7606(1989)101<1520:DSIASO>2.3.CO;2.

Cloos, M., 1982, Flow mélanges: Numerical modeling and geologic constraints on their origin in the Franciscan subduction complex: *Geological Society of America Bulletin*, v. 93, p. 330–345, doi: 10.1130/0016-7606(1982)93<330:FMNMAC>2.0.CO;2.

Cowan, D.S., 1985, Structural styles in Mesozoic and Cenozoic mélanges in the western Cordillera of North America: *Geological Society of America Bulletin*, v. 96, p. 451–462, doi: 10.1130/0016-7606(1985)96<451:SSIMAC>2.0.CO;2.

Cowan, D.S., and Page, B.M., 1975, Recycled Franciscan material in Franciscan mélange west of Paso Robles, California: *Geological Society of America Bulletin*, v. 86, p. 1089–1095.

Ernst, W.G., 1988, Tectonic history of subduction zones inferred from retrograde blueschist P - T paths: *Geology*, v. 16, p. 1081–1084, doi: 10.1130/0091-7613(1988)016<1081:THOSZL>2.3.CO;2.

Fisher, D., and Byrne, T., 1987, Structural evolution of underthrust sediments, Kodiak islands, Alaska: *Tectonics*, v. 6, p. 775–793, doi: 10.1029/TC006i006p00775.

Flinn, D., 1962, On folding during three-dimensional progressive deformation: *Geological Society of London Quarterly Journal*, v. 118, p. 385–433.

Guidotti, C.V., Sassi, F.P., and Blencoe, J.G., 1989, Compositional controls on the a and b cell dimensions of 2M1 muscovite: *European Journal of Mineralogy*, v. 1, p. 71–84.

Hashimoto, Y., and Kimura, G., 1999, Underplating process from mélange formation to duplexing: Example from the Cretaceous Shimanto Belt, Kii Peninsula, southwest Japan: *Tectonics*, v. 18, p. 92–107, doi: 10.1029/1998TC900014.

Hibbard, J., Karig, D., and Taira, A., 1992, Anomalous structural evolution of the Shimanto accretionary prism at Murotomisaki, Shikoku Island, Japan: *The Island Arc*, v. 1, p. 133–147, doi: 10.1111/j.1440-1738.1992.tb00065.x.

Hsü, K.J., 1968, Principles of mélanges and their bearing on the Franciscan-Knoxville paradox: *Geological Society of America Bulletin*, v. 79, p. 1063–1074, doi: 10.1130/0016-7606(1968)79[1063:POMATB]2.0.CO;2.

Ikesawa, E., Kimura, G., Sato, K., Ikehara-Ohmori, K., Kitamura, Y., Yamaguchi, A., Ujiie, K., and Hashimoto, Y., 2005, Tectonic incorporation of the upper part of oceanic crust to overriding plate of a convergent margin: An example from the Cretaceous–early Tertiary Mugi mélange, the Shimanto Belt, Japan: *Tectonophysics*, v. 401, p. 217–230, doi: 10.1016/j.tecto.2005.01.005.

Ishida, S., 1969, Wano Formation (Eocene) in Amami Oshima, Ryukyu Island, Japan: *Journal of the Geological Society of Japan*, v. 75, p. 141–156.

Kanisawa, S., Osozawa, S., and Nakagawa, H., 1983, Petrology of Mesozoic lamprophyres in Amami-Oshima, Kagoshima Prefecture, Japan: *Journal of Mineralogy, Petrology, and Economic Geology*, v. 78, p. 394–404.

Kimimami, K., Miyashita, S., and Kawabata, K., 1994, Ridge collision and in-situ greenstones in accretionary complexes: The Island Arc, v. 3, p. 103–111, doi: 10.1111/j.1440-1738.1994.tb00098.x.

Kimura, G., and Mukai, A., 1991, Underplated units in an accretionary complex: Mélange of the Shimanto Belt of eastern Shikoku, southwest Japan: *Tectonics*, v. 10, p. 31–50, doi: 10.1029/90TC00799.

Kübler, B., 1968, Evaluation quantitative du métamorphisme par la cristallinité de l'illite: *Bulletin du Centre de Recherche de Pau-Société Nationale des Pétales d'Aquitaine*, v. 2, p. 385–397.

Lucente, C.C., and Pini, G.A., 2003, Anatomy and emplacement mechanism of a large submarine slide within a Miocene foredeep in the Northern Apennines, Italy: A field perspective: *American Journal of Science*, v. 303, p. 565–602, doi: 10.2475/ajs.303.7.565.

Matsuda, S., and Ogawa, Y., 1993, Two-stage model of incorporation of seamount and oceanic blocks into sedimentary mélange: Geochemical and biostratigraphic constraints in Jurassic Chichibu accretionary complex, Shikoku, Japan: *The Island Arc*, v. 2, p. 7–14, doi: 10.1111/j.1440-1738.1993.tb00071.x.

Needham, D.T., 1987, Asymmetric extensional structures and their implications for the generation of mélanges: *Geological Magazine*, v. 124, p. 311–318.

Onishi, T.C., and Kimura, 1995, Change in fabric of mélange in the Shimanto Belt, Japan: Change in relative convergence?: *Tectonics*, v. 14, p. 1273–1289.

Orange, D.L., 1990, Criteria helpful in recognizing shear-zone and diapiric mélange: Examples from the Hoh accretionary complex, Olympic Peninsula, Washington: *Geological Society of America Bulletin*, v. 102, p. 935–951, doi: 10.1130/0016-7606(1990)102<0935:CHIRSZ>2.3.CO;2.

Osozawa, S., 1984, Geology of Amami Oshima, central Ryukyu Islands, with special reference to effect of gravity transportation on geologic structure: The Science Report of the Tohoku University, Sendai, Second Series (Geology), no. 54, p. 165–189.

Osozawa, S., 1986, Origin of chert, limestone and basalt complex in Japan: *Journal of the Geological Society of Japan*, v. 92, p. 709–722.

Osozawa, S., 1993, Normal faults in accretionary complex formed at trench-trench-ridge triple junction, as an indicator of angle between the trench and subducted ridge: *The Island Arc*, v. 2, p. 142–151, doi: 10.1111/j.1440-1738.1993.tb00082.x.

Osozawa, S., 2006, Mélanges and dikes of the Miocene Nabae complex, Muroto Peninsula, Shikoku, Japan, in Iwai, M., Murata, A., and Yoshimura, Y., eds., *Field Excursion Guide Book, 113th Annual Meeting of Geological Society of Japan: Kochi*, Geological Society of Japan, p. 41–53.

Osozawa, S., and Yoshida, T., 1997, Arc-type and intraplate-type ridge basalts formed at the trench-trench-ridge triple junction: Implication for the extensive sub-ridge mantle heterogeneity: *The Island Arc*, v. 6, p. 197–212, doi: 10.1111/j.1440-1738.1997.tb00170.x.

Osozawa, S., Sakai, T., and Naito, T., 1990, Miocene subduction of an active mid-ocean ridge and origin of the Setogawa ophiolite: *The Journal of Geology*, v. 98, p. 763–771.

Osozawa, S., Takeuchi, H., and Koitabashi, T., 2004, Formation of the Yakuno ophiolite; accretionary-subduction under medium-pressure type metamorphic conditions: *Tectonophysics*, v. 393, p. 197–219, doi: 10.1016/j.tecto.2004.07.033.

Pini, G.A., 1999, Tectosomes and Olistostromes in the Argille Scagliose of the Northern Apennines, Italy: *Geological Society of America Special Paper* 335, 70 p.

Sassi, F.P., and Scolari, A., 1974, The b_0 value of the potassium white micas as a barometric indicator in low-grade metamorphism of pelitic schist: *Contributions to Mineralogy and Petrology*, v. 45, p. 143–152.

Schoonover, M., and Osozawa, S., 2004, Exhumation process of the Nago subduction related metamorphic rocks, Okinawa, Ryukyu island arc: *Tectonophysics*, v. 393, p. 221–240, doi: 10.1016/j.tecto.2004.07.036.

Taira, A., Okada, H., Whitaker, J.H.McD., and Smith, A.J., 1982, The Shimanto Belt, The b₀ value of the potassium white micas as a barometric indicator in low-grade metamorphism of pelitic schist: *Contributions to Mineralogy and Petrology*, v. 45, p. 143–152.

Schoonover, M., and Osozawa, S., 2004, Exhumation process of the Nago subduction related metamorphic rocks, Okinawa, Ryukyu island arc: *Tectonophysics*, v. 393, p. 221–240, doi: 10.1016/j.tecto.2004.07.036.

Taira, A., Okada, H., Whitaker, J.H.McD., and Smith, A.J., 1982, The Shimanto Belt, The b₀ value of the potassium white micas as a barometric indicator in low-grade metamorphism of pelitic schist: *Contributions to Mineralogy and Petrology*, v. 45, p. 143–152.

Taira, A., Katto, J., Tashiro, M., Okamura, M., and Kodama, K., 1988, The Shimanto Belt in Shikoku, Japan: Evolution of Cretaceous to Miocene accretionary prism: *Modern Geology*, v. 12, p. 5–46.

Taira, A., Byrne, T., and Ashi, J., 1992, *Photographic Atlas of an Accretionary Prism: Geologic Structures of the Shimanto Belt, Japan*: Tokyo, University of Tokyo Press, 124 p.

Takeuchi, M., 1993, Geology of the Yuwan district, with Geological Sheet Map at 1:50,000: Tsukuba, Japan, Geological Survey of Japan, 69 p.

Toriumi, M., and Teruya, J., 1988, Tectono-metamorphism of the Shimanto Belt: *Modern Geology*, v. 12, p. 303–324.

Underwood, M.B., Laughland, M.M., and Kang, S.M., 1993, A comparison among organic and inorganic indicators of diagenesis and low-temperature metamorphism, Tertiary Shimanto Belt, Shikoku, Japan, in Underwood, M.B. ed., *Thermal Evolution of the Tertiary Shimanto Belt, Southwest Japan: An Example of Ridge-Trench Interaction*: *Geological Society of America Special Paper* 273, p. 45–62.

Wakita, K., 1988, Origin of chaotically mixed rock bodies in the early Cretaceous sedimentary complex of the Mino terrane, central Japan: *Bulletin of Geological Survey of Japan*, v. 39, p. 675–757.

Wakita, K., 2000, Mélanges of the Mino terrane: *Memoirs of Geological Society of Japan*, v. 55, p. 145–163.

Xenophontos, C., and Osozawa, S., 2004, Travel time of accreted igneous assemblages in Western Pacific orogenic belts and their associated sedimentary rocks: *Tectonophysics*, v. 393, p. 241–261, doi: 10.1016/j.tecto.2004.07.037.

MANUSCRIPT RECEIVED 10 MAY 2006
REVISED MANUSCRIPT RECEIVED 4 FEBRUARY 2008
MANUSCRIPT ACCEPTED 5 FEBRUARY 2008

Printed in the USA